

Effectiveness of Field Oriented Control and Direct Torque Control Methods for Induction Motor Speed Regulation

SOHAIL AHMAD, HA THU LE
Department of Electrical and Computer Engineering,
California State Polytechnic University, Pomona,
Pomona City, California 91768,
UNITED STATES OF AMERICA

Abstract: – Induction motors are used extensively in many sectors, including manufacturing, power generation, healthcare, and transportation. Robust speed regulation of inductor motors is a key requirement for ensuring their intended usage and increasing their effectiveness. This study analyzes two advanced and popular methods for regulating the torque and speed of induction motors, namely, field-oriented control (FOC) and direct torque control (DTC). Detailed mathematical modeling of both methods is described, providing the in-depth perspective of the control algorithms and problem variables. This is followed by a thorough analysis of the performance of the control methods. Different control scenarios have been analyzed using simulation with MATLAB Simulink under different speed and loading conditions. The outcomes show that FOC provides better performance in terms of reduced torque jitter, smooth torque, and speed tracking response for highly variable load and reference speed profiles. Further, the FOC is found to generate better current waveforms. This leads to improving the power factor, decreasing electrical noise, and enhancing the motor performance. Meanwhile, the DTC demonstrates a strong capability to handle large speed changes and provide faster torque response, but it suffers from considerable torque variation. The simulation outcomes also suggest that the method selected to tune PI controllers is effective. The findings contribute to enhancing the efficient operation of induction motors and fostering their applications in diverse sectors for improved productivity and service, and superior economic gain.

Key-Words: - Controller tuning, direct torque control, field-oriented control, induction motor, motor speed control, PI controller, torque jitter, vector control.

Received: December 1, 2023. Revised: December 20, 2023. Accepted: December 27, 2023. Published: December 31, 2023.

1 Introduction

Three-phase induction motors (IM) have established themselves as industrial workhorses. Their applications are diverse, and include power generation, manufacturing, healthcare, and multiple other sectors. One of the most important characteristics that make IM a ubiquitous choice in large-scale applications is versatility, efficiency, and reliability. Due to their direct influence on the performance of motors, efficient control techniques are vital to be used in their design schemes. Multiple control techniques have been developed for induction motors with various performances. Understanding the advantages and disadvantages of the control techniques is of great importance for correct application.

Induction machines are used as industrial drives for a variety of equipment, such as drilling machines, saws, conveyors, elevators, power tools, and robotics arms. Correct control of these motors is crucial to ensure the effective operation of industrial

equipment. A small variation in speed may cause faulty products, instability in driven equipment, discomfort for users, and lower effectiveness of manufacturing processes, [1], [2].

In efforts to reduce carbon emissions in the transportation sector, countries around the world have implemented policies and set goals to transition from gasoline-fueled to electric vehicles. Induction motors are used as drives in multiple electric vehicle models, [3], [4], [5], [6]. This is another stimulant for seeking effective methods to regulate induction motor speed. Electric motors must provide smooth driving by being able to accelerate and decelerate quickly in response to changes in road conditions, as well as in compliance with traffic rules. Further, they must efficiently use energy to extend the vehicle range, [7], [8], [9], [10].

Another important application of induction machines is found in renewable energy areas, including wind power generation (wind farms),

solar PV, and concentrating solar plants. Here, again, speed control plays a critical role. Induction machines are used as generators in wind turbines. Additionally, they are used as motors to drive supporting systems in wind turbines, such as blade pitching drive and yaw drive. Solar PV systems use sun trackers to maximize their energy capture where induction motors are the system drives. Accurate control of the motors is key for efficient operation of the wind turbines and the solar trackers.

Health care is another sector where induction machines play an important role. One example is Magnetic Resonance Imaging (MRI) equipment where correct control of motor speed is a must for the system to function properly. Another example is infusion pumps which rely on precise motor control for correct administration of fluid and medicine for patients.

The above analysis and examples suggest an increasingly important role of induction machines which goes beyond industrial and manufacturing sectors to reach other critical areas, such as transportation, renewable energy, and healthcare. It motivates us to conduct a study to analyze some advanced control methods to obtain a better understanding of their characteristics and performance. The study findings are expected to contribute to the ongoing progress of motor control, increasing efficiency and fostering diverse applications of induction machines.

First, our study will provide a brief literature review of important induction motor speed control methods. Then, we will focus on analyzing two recent and popular control methods, namely Field-Oriented Control and Direct Torque Control, concerning their precision, torque and speed behaviors, and related characteristics. The analysis is performed using MATLAB Simulink and a realistic modeling motor and control system.

1.1 Voltage-Frequency Control (V/f Control)

Voltage-Frequency control, also known as scalar control or V/f control, is a powerful method for regulating the speed of induction motors. It involves changing the motor supply voltage magnitude and frequency simultaneously. By doing so, the motor speed can be regulated without impacting the motor's maximum torque capability. There are different ways where the V/f ratio is varied to provide a special operating performance. The most common method is fixed, or constant, V/f ratio. V/f control methods can maintain constant speed across a wide range of loads. However, they may not suit all applications that require variable speed operation

and may lack the precision required for demanding applications, [8], [9], [10], [11], [12].

1.2 Vector Control (Field-Oriented Control)

Field-Oriented Control (FOC) is an advanced vector control technique, which is widely used for induction motor speed control. The core of the FOC method involves decomposing motor stator current into a magnetic field-generating part and a torque-generating part. These current components are then controlled separately using PI controllers to obtain desirable speeds and performance. FOC implementation requires expensive sensors and a complex control algorithm. Though, it is capable of high-performance motor control with smooth rotation over the entire speed range, as well as fast acceleration and deceleration, [10], [11], [12], [13].

1.3 Direct Torque Control (DTC)

Direct torque control (DTC) is another advanced vector control method. It involves estimating (decoupling) motor magnetic flux and torque using measured voltage and current. The estimated flux and torque are compared with their reference values. If the estimated flux or torque deviates far the reference values, the motor variable speed drive (VFD) is operated to bring the flux and torque errors within their tolerance bands as quickly as possible. An advantage of DTC is that torque and flux can be changed very fast by altering the references. Further, there is no need for PI current controllers. The VFD operates electronic switches to reduce flux and torque errors. However, DTC needs highly accurate voltage and current measurements, which may be difficult to obtain. In addition, the control equipment must be very fast to prevent the flux and torque from deviating far from the tolerance bands. Hence, DTC requires a complex motor model and complex control algorithms while potentially having considerable torque ripple, [14], [15], [16], [17], [18], [19], [20], [21], [22], [23].

1.4 Sensorless Control

Many induction motor speed control systems require speed and position sensors, such as absolute encoders and magnetic resolvers. These sensors can be expensive and require frequent maintenance. Sensorless control techniques, such as sensorless vector control and back EMF estimation, do not require sensors. Advantages of sensorless motor drives include reduced cost, increased reliability, lower complexity of drive circuits, and less maintenance requirement. Sensorless methods utilize the estimation of motor model parameters and are employed in applications where sensors are

either unsuitable or too expensive, [22], [24], [25], [26].

1.5 Sliding Mode Control

Sliding mode control (SMC) is a nonlinear control method that, by applying a set-valued control signal, forces the controlled system (such as an induction motor) to "slide" along a cross-section of the system's normal behavior. SMC may be viewed as a special case of a hybrid dynamical system because the system flows through a continuous state space while moving through different discrete control modes. SMC can keep the intended motor speed constant under disturbance conditions, thanks to its superior capability to handle disturbance and uncertainty. This is achieved by constructing a "sliding surface" on which the motor's state variables converge to desirable values. However, in some applications, SMC may produce high harmonics and cause acoustic noise, [15], [19], [25], [27], [28], [29], [30].

The following sections present an investigation of FOC and DTC, the two advanced and popular vector control methods. The goal is to obtain a better understanding of their torque and speed behaviors, related characteristics, and effectiveness in regulating the induction motor speed.

2 Analysis of Field Oriented Control of Induction Motor

As said previously, the core of the FOC method involves decomposing motor stator current into a magnetic field-generating part and a torque-generating part. These components are then controlled separately using PI current controllers to achieve desirable speeds and performance. The following section presents FOC mathematical representations that underline it.

2.1 Variable Frequency Drive, [31], [32]

The induction motor speed is regulated using a Variable Frequency Drive, which changes the magnitude and frequency of the voltage applied to the motor. This adjustment is critical to achieve optimal motor performance, efficiency, and responsiveness.

$$V_s = V_m \sin(\omega t) \quad (1)$$

where V_s , V_m and ω are the source voltage, maximum voltage, and angular frequency, respectively.

2.2 Clarke Transformation, [31], [32]

Clarke transformation is used to transform the motor stator phase currents, I_a , I_b , and I_c , into the alpha-beta frame. This transformation converts the three-phase currents into two-phase currents, simplifying the control of the motor in a two-dimensional frame.

$$\begin{aligned} I_\alpha &= I_a \\ I_\beta &= \frac{\sqrt{3}}{2} I_a + \frac{1}{2} I_b \end{aligned} \quad (2)$$

2.3 Park Transformation, [31], [32]

As a next step in the control process, after Clark transformation, the alpha-beta frame currents are transformed into dq-coordinates using Park transformation. Park transformation decouples the active and reactive power components (a magnetic field-generating part and a torque-generating part), making it possible to control them independently.

2.4 Slip Speed Estimation and Position Generation

The speed feedback from the motor is added to the slip speed estimator. This estimator block determines the slip speed by taking the reference stator current in the dq frame:

$$s = \frac{\omega_s - \omega_r}{\omega_s} \quad (3)$$

where, s , ω_r and ω_s represent the slip, synchronous, and rotor speeds respectively.

The estimated slip speed is then summed and fed to the position generator to generate the angle which is input to the Park transform block and influences the dq currents for control.

2.5 PI Controller for FOC Control Block

The PI controller's objective is to maintain the speed and current within their frames. The controller inputs are motor currents and speed while the output is the duty cycle for the two-level converter.

2.6 Implementation

Error calculation: The error is computed as the difference between the desired and actual motor torque or flux.

PID controller operation: For each sampling period

- Compute the proportional term as P multiplied by the error.
- Compute the integral term by accumulating the error over time and then multiplying by I.
- Compute the derivative term by determining the change in error from the last period and then multiplying by D.
- Duty cycle computation: Combine the P, I, and D outputs to determine the inverter duty cycle.

2.7 Performance and Adjustment

After initial tuning, it is crucial to evaluate system performance. If overshooting or slow system response occurs, make necessary adjustments to the PID parameters:

- If the system oscillates, the P gain might be too high.
- If the system responds slowly, the P gain might be too low or the I gain too high.
- If the system overshoots and takes a while to settle, the D gain might need adjustment.

2.8 Tuning Methodology

Various tuning methodologies exist, but for the purpose of this study, the following PID control tuning method as explained in the following study was used.

The methodology is explained as, Setting Gain Controls for the FOC Algorithm. The regulator gains are calculated by the implementation of the pole-zero cancellation technique. This methodology has the main advantage over other systems as it does not influence the order of the system. The inner loop transfer function of the controller is given using the following equation, [31], [32].

$$\frac{i_{sa}}{i_{sa-ref}} = K_{P(\alpha)-I} \cdot b \quad (4)$$

$$\frac{K_{I(\alpha)-I}}{K_{P(\alpha)-I}} = a_5$$

Similarly, the outer loop transfer function of the controller is tuned as,

$$\frac{\varphi_r}{\varphi_{r-ref}} = \frac{K_{P(\alpha)-\varphi_r} \cdot K_{P(\alpha)-I} \cdot b \cdot a_2}{s^2 + K_{P(\alpha)-I} \cdot b \cdot s + K_{P(\alpha)-\varphi_r} \cdot K_{P(\alpha)-I} \cdot b \cdot a_2} \quad (5)$$

$$a_1 = \frac{K_{I(\alpha)-\varphi_r}}{K_{P(\alpha)-\varphi_r}}$$

All other relevant equations are given in [31], [32]. The calculations for Kp and Ki are done for the following constant values in the motor.

All these values were substituted into the above equations with the values of a1, a2, a3, a4 and a5 calculated as,

$$a_1 = \frac{R_r}{L_r} \quad (6)$$

$$a_2 = \frac{L_m R_r}{L_r} \quad (7)$$

$$a_3 = \frac{L_m R_r}{\sigma L_s L_r^2} \quad (8)$$

$$a_4 = \frac{L_m}{\sigma L_s L_r} \quad (9)$$

$$a_5 = L_r^2 R_s + \frac{L_m^2 R_r}{\sigma L_s L_r^2}, b = \frac{1}{\sigma L_s} \quad (10)$$

$$\sigma = 1 - \frac{L_m^2}{L_s L_r} \quad (11)$$

Table 1. Constant parameters of induction motor used for testing the control algorithm, [31]

Parameters	Values
Supply Voltage (V)	460 V
Power (kW)	111.85 kW/150 HP
Stator Resistance (Rs)	0.0302 ohm
Rotor Resistance (Rr)	0.01721 ohm
Stator Inductance (Ls)	0.000283 H
Rotor Inductance (Lr)	0.000283 H
Mutual Inductance (Lm)	0.01095 H
Inertia (J)	2
Friction Factor (f)	0.0
Pole Pairs (p)	2
Frequency (F)	60 Hz
Nominal Speed (rad/sec)=2*pi*f	376.9914 rad/sec
Nominal Torque (Nm)=9.548*Power/N	600 Nm

Table 2. Calculated parameters for tuning PI controller coefficients, [32]

Constants for calculating control parameters used in the study	
a1	14.28
a2	60.25
a3	-137.819
a4	-6.414e-4
a5	20

Table 3. Tuned PI regulator parameters for current control

Control Parameters	
Kp	Ki
0.15	3
0.1	2
0.05	1
0.02	0.4
0.01	0.2

Table 4. Tuned PI regulator parameters for voltage control

Control Parameters	
Kp	Ki
450	6426
320	4569
260	3714
200	2857
140	2000

Calculation of gains for current controller

$$k_{I_{current}} = k_{p_{current}} a_5 \quad (12)$$

where Kp can be assumed.

Calculation of gains for speed controller

$$k_{I_{flux}} = k_{p_{flux}} a_1 \quad (13)$$

where Kp can be tuned by trial-and-error as in the current controller. The values of Kp were assumed and the best value was taken in terms of response.

2.9 Simulation Results for FOC

The FOC diagram is shown in Figure 1 and the control method is implemented using MATLAB Simulink (Figure 2) to regulate the speed of an IM. Table 1, Table 2, Table 3 and Table 4 contain induction motor and PI controller parameters for the FOC simulation. The simulation data are also provided in Table A1, Table A2, Table A3 and Table A4 of Appendix for reader convenient reference. Various simulation scenarios are considered. The goal is to better understand the behavior of torque in relation to variation in reference speed for the controller. Different set points were analyzed in the final assessment of the designed model. The reference speed (ω_{ref}) in rpm, reference flux (ϕ_{ref}) in V_s , and reference torque and current are represented in different subplots.

The simulations were done by varying the motor speed at different time instants, namely, 0, 1.5, and 2.5 seconds. The reference speed was set at 1785rpm, 1500rpm, and 500 rpm, respectively. The IM is run at different load torque values, namely 50%, 60%, 70%, 80%, 90%, and 100% of the

nominal torque. The results are presented in Figure 3, Figure 4, Figure 5, Figure 6, Figure 7 and Figure 8.

As evident Figure 3, Figure 4, Figure 5, Figure 6, Figure 7 and Figure 8, all the reference and set points were very efficiently tracked by the controller and the current drawn by the motor is also free from any non-sinusoidal components. Since the simulation was run for a significant time, the flux tracking was also achieved with a very smooth and critically damped response. The results demonstrated that the model contained all these discussed characteristics and performed better than any other contemporary or even better models.

Analysis of motor behavior of Figure. 3:

Initially, the motor draws a larger current (bottom plot) than its rated value due to low torque at start-up. The motor runs a load magnitude equating to 50% of its rated value. Once the motor attains its rated speed, the in-rush current is stabilized. This current remains constant unless the speed or torque requirements are varied. This is evident from the time stamp ranging from 1.5s to 1.6s where the speed is varied and consequently, the torque is also changed. The overshoot during these changes remained within permissible limits of 2% which advocates the significance of the PI controller tuning.

The first plot of Figure 3 (speed) shows that the motor speed follows the reference speed closely. The 3rd plot (torque) shows that the torque produced by the motor (Blue) matches the Reference torque generated by the controller (Light Yellow, not visible as it is obscured by the Blue curve) in response to variable speed command. The motor torque waveform has some variation, but the average value is relatively stable. In the meantime, load torque (Dark Yellow) is maintained at two constant values. The initial load is set lower to enable the motor to start and accelerate.

Analysis of motor behavior of Figure 4, Figure 5, Figure 6, Figure 7 and Figure 8:

We observe similar behavior as that of Figure 3 in terms of current, speed, and torque when the motor is run at 60%, 70%, 80%, 90%, and 100% of its rated load value. The motor speed follows the reference speed closely. The motor produced torque matches the Reference torque generated by the controller.

Overall, the outcomes of Figure 3, Figure 4, Figure 5, Figure 6, Figure 7 and Figure 8 suggest that the FOC-based control system can regulate the

motor speed over a wide range of loading in a steady and smooth manner.

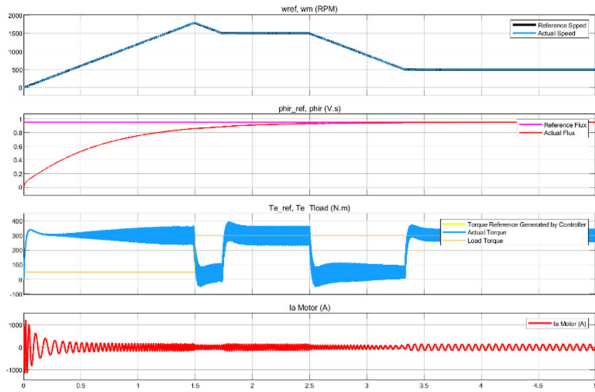


Fig. 3: Results at 50% nominal torque (FOC)

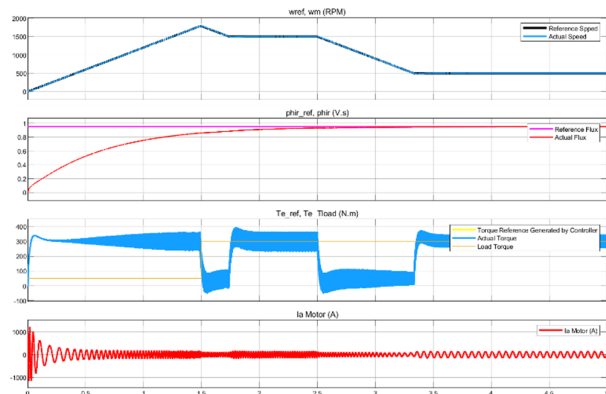


Fig. 4: Results at 60% nominal torque (FOC)

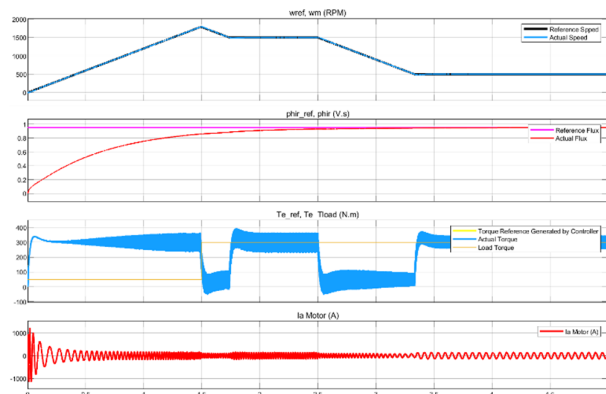


Fig. 5: Results at 70% nominal torque (FOC)

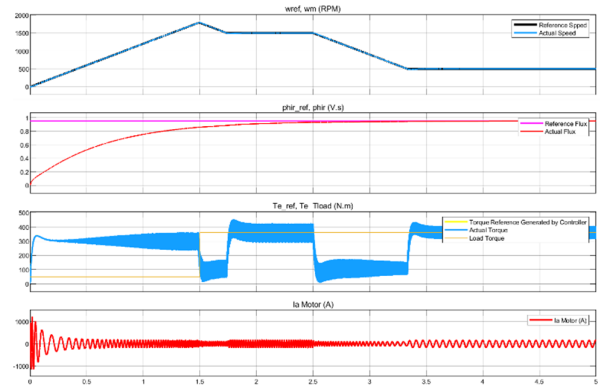


Fig. 6: Results at 80% nominal torque (FOC)

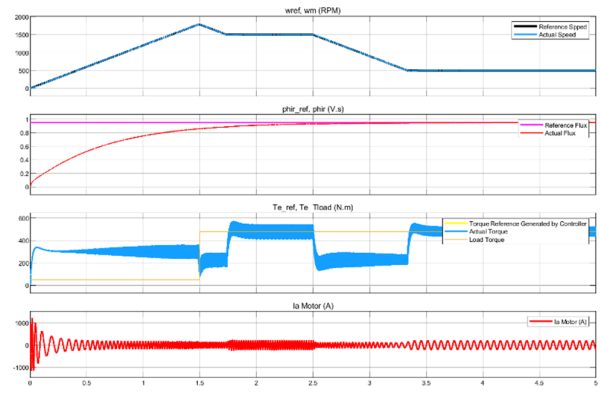


Fig. 7: Results at 90% nominal torque (FOC)

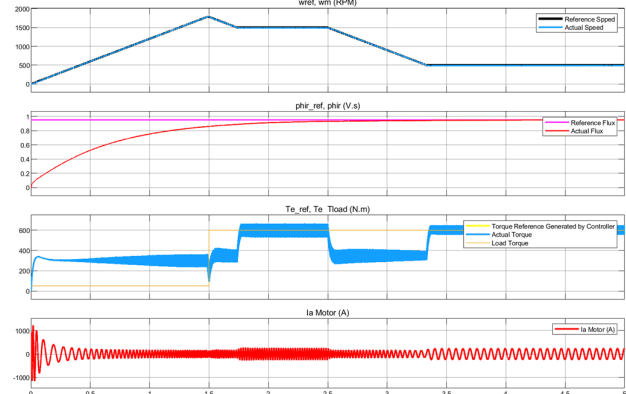


Fig. 8: Results at 100% nominal torque (FOC)

3 Analysis of Direct Torque Control of Induction Motor

Because of its fast dynamic reaction and lower complexity when compared to the field-oriented control method, Direct Torque Control (DTC) is a common control method for induction motors. A DTC diagram is shown in Figure 9 and a brief explanation of the DTC mathematical model is presented below.

3.1 Induction Motor Modeling, [32], [33]

The mathematical model of an induction motor is given by the following equations.

$$v_{s\alpha} = R_s i_{s\alpha} + \frac{d}{dt} \lambda_{s\alpha} \quad (14)$$

$$v_{s\beta} = R_s i_{s\beta} + \frac{d}{dt} \lambda_{s\beta} \quad (15)$$

Where the subscript s represents stator and v and i represent voltage and current respectively. R is the resistance, and the flux linkage is represented by λ .

3.2 Stator Flux Modeling, [32], [33]

The modeling of stator flux linkage can be represented using the following equations.

$$\lambda_{s\alpha} = L_s i_{s\alpha} + L_r i_{r\alpha} \quad (16)$$

$$\lambda_{s\beta} = L_s i_{s\beta} + L_r i_{r\beta} \quad (17)$$

3.3 Torque and Flux Modeling, [32], [33]

The following equations approximate the torque produced by the motor.

$$T_e = \frac{3p}{2} (\lambda_{s\beta} i_{s\alpha}) - (\lambda_{s\alpha} i_{s\beta}) \quad (18)$$

3.4 Procedure for Implementation of the Control Algorithm, [32], [33]

The primary idea behind DTC is to use the inverter's voltage vector to manage the stator flux and torque within their respective hysteresis regions.

- Examine the estimated torque and stator flux in relation to their reference values.
- Using a lookup table, select the appropriate voltage vector to change the stator flux and torque based on the inaccuracy.
- Use this voltage vector to run the motor via the inverter.

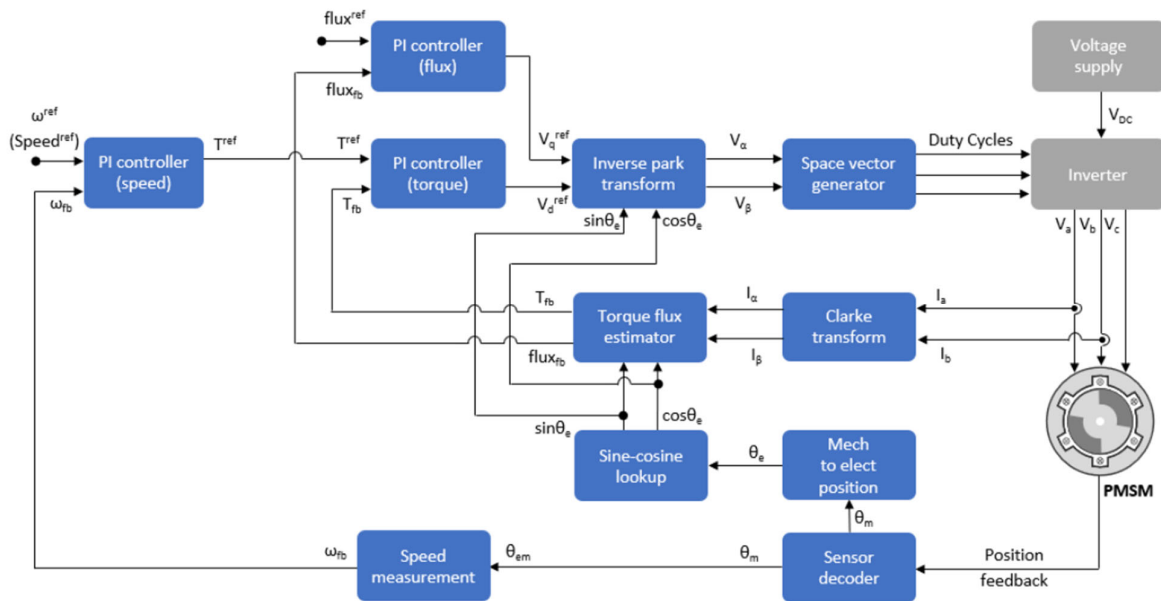


Fig. 9: Basic block diagram for Direct Torque Control (DTC) of induction motor, [33]

3.5 Simulation Results for DTC

The direct torque control method was also simulated using MATLAB Simulink (it is similar to that of Figure 2, not shown for brevity) for different torque loading conditions to obtain the controller responses. The speed of the motor was initially set equal to the rated speed and the torque varied between values ranging from 50%-100% of the rated value. Figure 10, Figure 11, Figure 12, Figure 13, Figure 14 and Figure 15 show the results. The reference parameters of speed (ω_{ref}), torque (T_{ref}), and current (I_{a_Motor}) are calculated in their SI units.

Analysis of motor behavior of Figure 10:

The inrush current in the case of the DTC method remained confined to a considerably lower value compared to the FOC method. This is evident from the 4th plot of Figure 10 where the motor runs at 50% of its nominal load. The inrush current almost remained in its rated limit with decreased frequency at starting. This decreased frequency is significant for a reduction in iron losses in the motor during start-up. Hence, the saturation point of the motor is also changed to a higher value due to this decreased frequency of inrush current.

As the motor runs at 50% of its rated load torque, the speed initially reaches the rated value of 1875 rpm. After that, the torque is stabilized and reaches its reference value of 300 Nm (Figure 10). The motor speed follows the varying speed command, as shown by the 1st plot of Figure 10. However, the motor-produced torque waveform has lots of ripples, as visible from the 3rd plot of Figure 10.

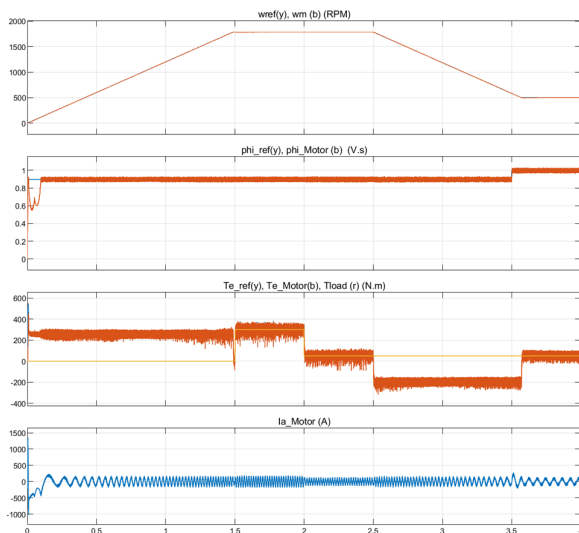


Fig. 10: Results at 50% nominal torque (DTC)

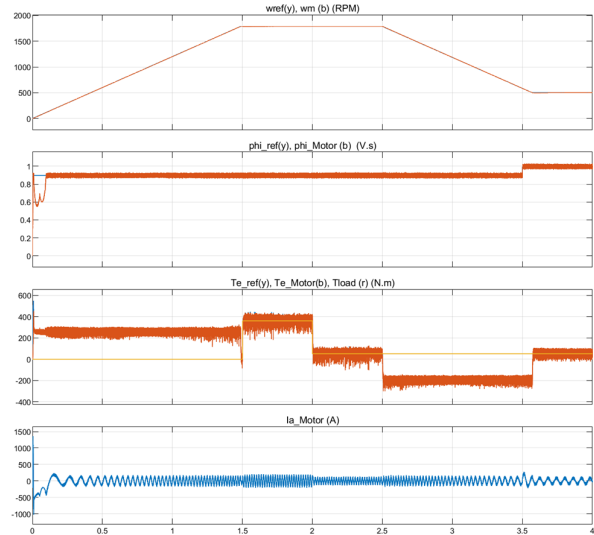


Fig. 11: Results at 60% nominal torque (DTC)

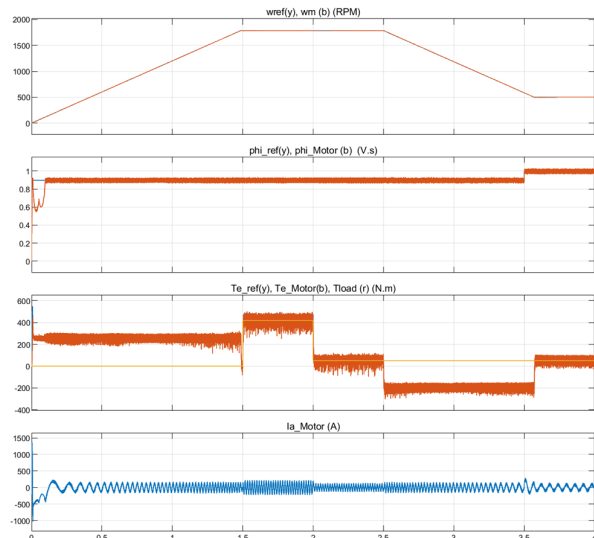


Fig. 12: Results at 70% nominal torque (DTC)

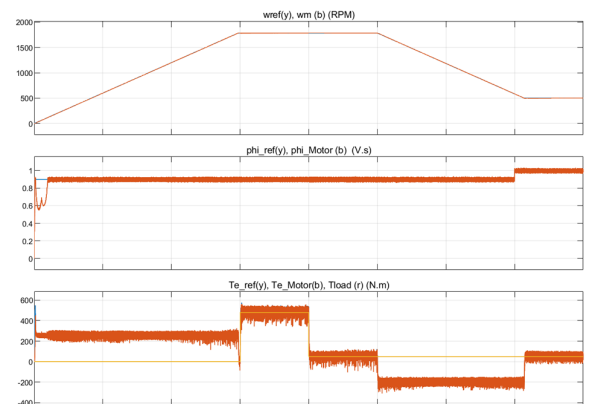


Fig. 13: Results at 80% nominal torque (DTC)

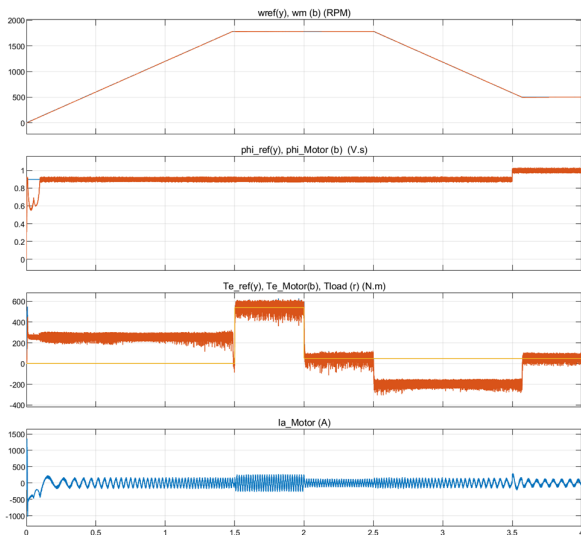


Fig. 14: Results at 90% nominal torque (DTC)

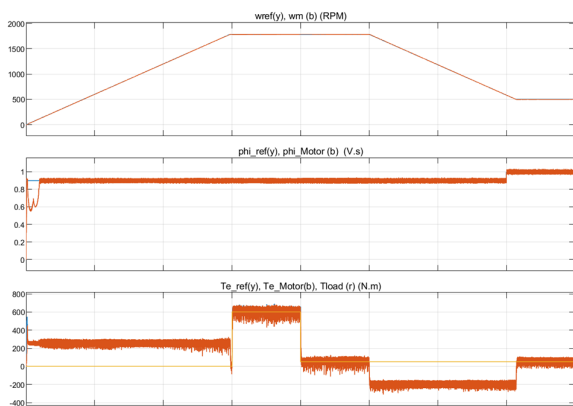


Fig. 15: Results at 100% nominal torque (DTC)

Analysis of motor behavior of Figure 11, Figure 12, Figure 13, Figure 14 and Figure 15:

A similar behavior is observed in terms of the motor speed and torque of the Figure 11, Figure 12, Figure 13, Figure 14, and Figure 15 where the motor is run at 60%, 70%, 80%, 90%, and 100% of its load torque. The motor follows the varying speed command closely. However, the motor has considerable torque jitter issues where the torque waveform has lots of variations and noise.

Notably, the DTC demonstrates an impressive capability to handle large speed changes. Taking Figure 14 as an example, at a 2.5s time stamp, the reference speed was decreased by 2.5 times from 1250 rpm to 500 rpm; the motor torque reduced almost immediately, facilitating the motor to decelerate to 500 rpm. As the motor speed reaches the desired value of 500 rpm at around 3.57s time stamp, the motor torque also stabilizes. Similar performance of the DTC is observed in Figure 10, Figure 11, Figure 12, Figure 13 and Figure 15.

4 Comparative Analysis of Advantages and Disadvantages of FOC and DTC Algorithms

Speed regulation under changing conditions:

The FOC algorithm performed exceptionally well in keeping precise and steady control in a variety of speed situations. This is an essential function, particularly in applications where fluctuating speed conditions are commonplace. For systems requiring high precision in speed control, the FOC is a more dependable option due to its strong regulation, which guarantees consistent performance.

However, DTC demonstrates a strong ability to handle large speed changes.

Torque jitter and harmonics:

FOC torque waveform shows noticeably lower levels of jitter and harmonics, as compared with that of DTC. This is another area where it excels over the DTC. Jitter, or the variations in torque seen in DTC, can result in mechanical strains and decreased motor operation efficiency. The ability of FOC to reduce these fluctuations results in longer equipment life, smoother motor operation, and higher system efficiency overall.

However, the DTC torque response is faster than that of FOC. To address the torque jitter issue, the current DTC could be combined with a secondary filter or another control algorithm. The suggested fixes could work to improve the effectiveness of the DTC technique.

Current waveforms:

For induction motors to operate efficiently, current waveform quality is essential. When compared to DTC, the FOC method was found to generate better current waveforms. This leads to improved power factor, decreased electrical noise, and enhanced motor performance. Better current waveforms also suggest less strain on the drive electronics and motor windings, which can result in longer motor life and lower maintenance costs.

5 Conclusion

The conducted study analyzes behaviors of two advanced and popular control methods, namely, Field-Oriented Control (FOC) and Direct Torque Control (DTC), for regulating the torque and speed of induction motors. First, the mathematical modeling of both methods is described. Then, diverse control scenarios are simulated using MATLAB Simulink. The outcomes have led to the following conclusion:

- a) Field Oriented Control provides better performance than Direct Torque Control in terms of reduced torque jitter. However, the DTC torque response is faster than that of the FOC.
- b) Both FOC and DTC provide good speed tracking responses for highly variable load and reference speed profiles. The FOC performs well in keeping precise and steady control in a variety of speed situations while the DTC demonstrates strong capability to handle large speed changes.
- c) Furthermore, the FOC algorithm is found to generate better current waveforms. This leads to improving the power factor, decreasing electrical noise, and enhancing the motor performance.
- d) The simulation outcomes show that the method that we selected and adjusted for tuning the PI controllers of FOC is effective. It can be used as a sample for engineers to tune similar controllers.

Overall, our study contributes some in-depth understanding of the core characteristics of FOC and DTC, namely, speed, torque, and current behaviors. It should be noted that tuning parameters of the PI controllers play a crucial role in ensuring proper functionality of the FOC-based control system. We contribute a sample of the tuning technique for tuning similar PI controllers. The study models are designed for the electrical requirements of the United States. However, the data can be extrapolated and used for other locations. The study findings are helpful for the operation of induction motors to increase their performance. They also foster applications of induction motors in diverse sectors for better productivity, enhanced service, and superior economic gain.

Acknowledgment:

The student author wants to acknowledge and thank Professor Ha Thu Le, the project advisor, for providing guidance and assistance throughout his master's study. Furthermore, the authors would like to thank the Master project committee members, Dr. Tim Lin and Dr. Dennis Fitzgerald, for their time and feedback.

References:

- [1] M. Drakaki, Y. L. Karnavas, I. A. Tzifettas, V. Linardos, and P. Tzionas, "Machine learning and deep learning based methods

- toward industry 4.0 predictive maintenance in induction motors: State of the art survey," *Journal of Industrial Engineering and Management (JIEM)*, vol. 15, no. 1, pp. 31–57, 2022, doi: 10.3926/JIEM.3597.
- [2] R. T. Novotnak, "A Systematic Approach to Selecting Flux References for Torque Maximization in Induction Motors," *IEEE Transactions on Control Systems Technology*, vol. 3, no. 4, pp. 388–397, 1995, doi: 10.1109/87.481963.
- [3] A. Carrillo, A. Pimentel, E. Ramirez, and H. T. Le, "Mitigating impacts of plug-in electric vehicles on local distribution feeders using a charging management system," *2017 IEEE Transportation and Electrification Conference and Expo, ITEC 2017*, pp. 174–179, Jul. 2017, doi: 10.1109/ITEC.2017.7993267.
- [4] T. Vo, J. Sokhi, A. Kim, and H. Thu Le, "Making Electric Vehicles Smarter with Grid and Home Friendly Functions," *2018 IEEE Transportation and Electrification Conference and Expo, ITEC 2018*, pp. 183–187, Aug. 2018, doi: 10.1109/ITEC.2018.8449949.
- [5] A. Kaiser, A. Nguyen, R. Pham, M. Granados, and Ha Thu Le, "Efficient Interfacing Electric Vehicles with Grid using Bi-directional Smart Inverter," *2018 IEEE Transportation and Electrification Conference and Expo, ITEC 2018*, pp. 714–719, Aug. 2018, doi: 10.1109/ITEC.2018.8450152.
- [6] J. Glueck and H. T. Le, "Impacts of Plug-in Electric Vehicles on local distribution feeders," *IEEE Power and Energy Society General Meeting*, vol. 2015-September, Sep. 2015, doi: 10.1109/PESGM.2015.7286348.
- [7] A. Z. Ahmad Firdaus, S. A. Azmi, K. Kamarudin, and M. H. B, "Review on different control techniques for induction motor drive in electric vehicle," *IOP Conference series: Materials Science and Engineering*, vol. 1055, no. 1, p. 012142, Feb. 2021, doi: 10.1088/1757-899X/1055/1/012142.
- [8] A.Z. Admad Firdaus, S. Azmi, K. Kamarudin, L.J. Hwai, H. Ali, M. Azalan, Z. Kasa, "Assessment of Control Drive Technologies for Induction Motor: Industrial Application to Electric Vehicle," *Journal of Physics: Conference Series*, vol. 1878, no. 1, Jun. 2021, doi: 10.1088/1742-6596/1878/1/012047.

- [9] A. Mehbodniya, P. Kumar, X. Changqing, J. L. Webber, U. Mamodiya, A. Halifa, and C. Srinivasulu, "Hybrid Optimization Approach for Energy Control in Electric Vehicle Controller for Regulation of Three-Phase Induction Motors," *Mathematical Problems in Engineering*, vol. 2022, 2022, doi: 10.1155/2022/6096983.
- [10] M. Ahmad, "Vector control of induction motor drives," *Power Systems*, vol. 30, pp. 47–75, 2010, doi: 10.1007/978-3-642-13150-9_3/COVER.
- [11] D. Benoudjit, M. S. Nait-Said, S. Drid, and N. Nait-Said, "On-line efficiency improvement of induction motor vector controlled," *Power Engineering and Electrical Engineering*, vol. 14, no. 3, pp. 247–253, Sep. 2016, doi: 10.15598/aece.v14i3.1682.
- [12] A. Achalhi, M. Bezza, N. Belbounaguia, and B. Boujoudi, "Improvement of Direct Torque Control by using a Space Vector Modulation Control of Three-Level Inverter," *IOP Conference Series: Materials Science and Engineering*, vol. 186, no. 1, Mar. 2017, doi: 10.1088/1757-899X/186/1/012025.
- [13] A. Kasbi and A. Rahali, "Performance evaluation of fractional character vector control applied for doubly fed induction generator operating in a network-connected wind power system," *Fractional-Order Modeling of Dynamic Systems with Applications in Optimization, Signal Processing, and Control*, pp. 179–211, Nov. 2021, doi: 10.1016/B978-0-32-390089-8.00012-X.
- [14] D. D. Kumar and N. P. Kumar, "Dynamic torque response improvement of direct torque controlled induction motor," *Journal of Physics: Conference Series*, vol. 1706, no. 1, Dec. 2020, doi: 10.1088/1742-6596/1706/1/012100.
- [15] A. Ammar, A. Bourek, and A. Benakcha, "Robust SVM-direct torque control of induction motor based on sliding mode controller and sliding mode observer," *Frontiers in Energy*, vol. 14, no. 4, pp. 836–849, Dec. 2020, doi: 10.1007/S11708-017-0444-Z/METRICS.
- [16] K. K. Shyu, J. K. Lin, V. T. Pham, M. J. Yang, and T. W. Wang, "Global minimum torque ripple design for direct torque control of induction motor drives," *IEEE Transactions on Industrial Electronics*, vol. 57, no. 9, pp. 3148–3156, Sep. 2010, doi: 10.1109/TIE.2009.2038401.
- [17] T. Rekioua and D. Rekioua, "Direct torque control strategy of permanent magnet synchronous machines," *2003 IEEE Bologna PowerTech - Conference Proceedings*, vol. 2, pp. 861–866, 2003, doi: 10.1109/PTC.2003.1304660.
- [18] G. Noriega, "Direct Torque Control of a Permanent Magnet Synchronous Motor using Fuzzy Logic." Jan. 01, 2007, [Online]. https://www.academia.edu/27114526/Direct_Torque_Control_of_a_Permanent_Magnet_Synchronous_Motor_using_Fuzzy_Logic (Accessed Date: August 22, 2023).
- [19] C. Lasca, A. Argeseanu, and F. Blaabjerg, "Supertwisting Sliding-Mode Direct Torque and Flux Control of Induction Machine Drives," *IEEE Transactions on Power Electronics*, vol. 35, no. 5, pp. 5057–5065, May 2020, doi: 10.1109/TPEL.2019.2944124.
- [20] N. P. Gupta and P. Gupta, "Performance analysis of direct torque control of PMSM drive using SVPWM - Inverter," *India International Conference on Power Electronics, IICPE*, 2012, doi: 10.1109/IICPE.2012.6450421.
- [21] N. E. Ouanjli, A. Derouich, A. E. Ghzizal, S. Motahhir, A. Chebabhi, Y. E. Mourabit, M. Taoussi, "Modern improvement techniques of direct torque control for induction motor drives-A review," *Protection and Control of Modern Power Systems*, vol. 4, no. 1, pp. 1–12, Dec. 2019, doi: 10.1186/S41601-019-0125-5/TABLES/2.
- [22] N. Farid, B. Sebti, K. Mebarka, and B. Tayeb, "Performance Analysis of Field-Oriented Control and Direct Torque Control for Sensorless Induction Motor Drives", *2007 Mediterranean Conference on Control & Automation*, 2007, pp.1-6.
- [23] L. Feng, X. Sun, X. Tian, and K. Diao, "Direct Torque Control with Variable Flux for an SRM Based on Hybrid Optimization Algorithm," *IEEE Transactions on Power Electronics*, vol. 37, no. 6, pp. 6688–6697, Jun. 2022, doi: 10.1109/TPEL.2022.3145873.
- [24] Z. Yin, F. Gao, Y. Zhang, C. Du, G. Li, and X. Sun, "A Review of Nonlinear Kalman Filter Applying to Sensorless Control for AC Motor Drives," *CES Transactions on Electrical Machines and Systems*, vol. 3, no.

- 4, pp. 351–362, Dec. 2019, doi: 10.30941/CESTEMS.2019.00047.
- [25] M. Zhou, S. Cheng, Y. Feng, W. Xu, L. Wang, and W. Cai, “Full-Order Terminal Sliding-Mode-Based Sensorless Control of Induction Motor With Gain Adaptation,” *IEEE Journal of Emerging and Selected Topics in Power Electronics*, vol. 10, no. 2, pp. 1978–1991, Apr. 2022, doi: 10.1109/JESTPE.2021.3081863.
- [26] H. Wang, Y. Yang, X. Ge, Y. Zuo, Y. Yue, and S. Li, “PLL- And FLL-Based Speed Estimation Schemes for Speed-Sensorless Control of Induction Motor Drives: Review and New Attempts,” *IEEE Transactions on Power Electronics*, vol. 37, no. 3, pp. 3334–3356, Mar. 2022, doi: 10.1109/TPEL.2021.3117697.
- [27] C. Laoufi, Z. Sadoune, A. Abbou, and M. Akherraz, “New model of electric traction drive based sliding mode controller in field-oriented control of induction motor fed by multilevel inverter,” *International Journal of Power Electronics and Drive System (IJPEDS)*, vol. 11, no. 1, pp. 242–250, 2020, doi: 10.11591/ijpeds.v11.i1.pp242-250.
- [28] I. Abadlia, M. Adjabi, and H. Bouzeria, “Sliding mode based power control of grid-connected photovoltaic-hydrogen hybrid system,” *International Journal of Hydrogen Energy*, vol. 42, no. 47, pp. 28171–28182, Nov. 2017, doi: 10.1016/J.IJHYDENE.2017.08.215.
- [29] A. J. Abianeh and F. Ferdowsi, “Sliding Mode Control Enabled Hybrid Energy Storage System for Islanded DC Microgrids with Pulsing Loads,” *Sustain Cities Soc*, vol. 73, p. 103117, Oct. 2021, doi: 10.1016/J.SCS.2021.103117.
- [30] S. Ahmad, J. Qi, A. Rasool, E. U. Rahman, S. Jobaer, M. A. Baig, A. Rahman, S. U. Din, “Terminal Sliding Mode Control (TSMC) Scheme for Current Control of Five-Phase Induction Motor,” *2020 3rd International Conference on Power and Energy Applications, ICPEA 2020*, pp. 121–124, Oct. 2020, doi: 10.1109/ICPEA49807.2020.9280133.
- [31] “Field-oriented control- Develop field-oriented control algorithms using simulation”, Mathworks, [Online]. <https://www.mathworks.com/solutions/electrification/field-oriented-control.html> (Accessed Date: February 1, 2024).
- [32] M. Elgbaily, F. Anayi, and M. M. Alshbib, “A Combined Control Scheme of Direct Torque Control and Field-Oriented Control Algorithms for Three-Phase Induction Motor: Experimental Validation,” *Mathematics* 2022, vol. 10, no. 20, p. 3842, Oct. 2022, doi: 10.3390/MATH10203842.
- [33] “Direct Torque Control, Mathworks”, [Online]. <https://www.mathworks.com/help/mcb/gs/direct-torque-control-dtc.html> (Accessed Date: February 1, 2024).

APPENDIX

Data used for MATLAB Simulink FOC simulation

The simulations were completed for specific motor data and the results can be extrapolated for further applications in different other schemes. The main parameters used in the study are given in the following tables.

Table A1. Constant parameters of induction motor used for testing the control algorithm, [31]

Parameters	Values
Supply Voltage (V)	460 V
Power (kW)	111.85 kW/150 HP
Stator Resistance (Rs)	0.0302 ohm
Rotor Resistance (Rr)	0.01721 ohm
Stator Inductance (Ls)	0.000283 H
Rotor Inductance (Lr)	0.000283 H
Mutual Inductance (Lm)	0.01095 H
Inertia (J)	2
Friction Factor (f)	0.0
Pole Pairs (p)	2
Frequency (F)	60 Hz
Nominal Speed (rad/sec)= $2\pi f$	376.9914 rad/sec
Nominal Torque (Nm)= $9.548 \cdot \text{Power}/N$	600 Nm

Table A2. Calculated parameters for tuning PI controller coefficients, [32]

Constants for calculating control parameters used in the study	
a1	14.28
a2	60.25
a3	-137.819
a4	-6.414e-4
a5	20

Table A3. Tuned PI regulator parameters for current control

Control Parameters	
Kp	Ki
0.15	3
0.1	2
0.05	1
0.02	0.4
0.01	0.2

Table A4. Tuned PI regulator parameters for voltage control

Control Parameters	
Kp	Ki
450	6426
320	4569
260	3714
200	2857
140	2000

Contribution of Individual Authors to the Creation of a Scientific Article (Ghostwriting Policy)

- Sohail Admad: Identification of research issues, system data acquisition, design and implementation, simulation, writing an original draft, and revising.
- Ha Thu Le: Refining research issues and scope, methodology, technical advising, refining simulation scenarios, review of results, formatting and editing the final draft, revising the reviewed paper to meet publisher requirements.

Sources of Funding for Research Presented in a Scientific Article or Scientific Article Itself

No funding was received for conducting this study.

Conflict of Interest

The authors declare that they have no known competing financial interests or personal relationships that could have appeared to influence the work reported in this paper.

Creative Commons Attribution License 4.0 (Attribution 4.0 International, CC BY 4.0)

This article is published under the terms of the Creative Commons Attribution License 4.0

https://creativecommons.org/licenses/by/4.0/deed.en_US